IPPI

Polyolefins Journal, Vol. 4, No. 2 (2017)
DOI: 10.22063/poj.2016.1418

ORIGINAl PAPER

Preparation and characterization of polyethylene/ glass fiber composite membrane prepared via thermally induced phase separation method

Ali Behboudi[1,2], Yoones Jafarzadeh[1,2*], Reza Yegani[1,2], Ali Akbari[1,2]

[1]Faculty of Chemical Engineering, Sahand University of Technology, Tabriz, Iran
[2]Membrane Technology Research Center, Sahand University of Technology, Tabriz, Iran

Received: 11 September 2016, Accepted: 24 December 2016

ABSTRACT

Grinded glass fiber (GGF) embedded high density polyethylene (HDPE) membranes were prepared via thermally induced phase separation method. FESEM images showed that all the membranes had leafy structure, indicating a solid-liquid mechanism during phase separation. The results of EDX and TGA analyses confirmed that the fibers were dispersed in the HDPE matrix uniformly. Normalized water flux of the membranes increased from 1 for the neat HDPE membrane to more than 4 for 10 wt% GGF/HDPE membrane. Moreover, the contact angle decreased from 129° to 94° as the GGF content increased in the membranes, showing an improvement in the surface hydrophilicity of the membranes. The AFM results revealed that the surface roughness of the membranes was increased with increasing the GGF content. The results of abrasion test revealed that the GGF/HDPE membranes had a more abrasion resistance than the neat HDPE membrane. Finally, the fouling behavior of the membranes was investigated by the filtration of BSA protein solution and the results showed that with increasing the glass fiber content, total fouling ratio decreased from 90% for the neat HDPE membrane to 62% for 10 wt% GGF/HDPE membrane, indicating that the antifouling properties of the membranes were improved due to the presence of glass fiber. **Polyolefins J (2017) 4: 201-212**

Keywords: Polyethylene; glass fiber; thermally induced phase separation (TIPS); abrasion; membrane fouling.

INTRODUCTION

Nowadays, membrane based processes are applied in various fields including gas separation, water and wastewater treatment, dairy products, pharmaceutical and chemical industries. The most important application of industrial membranes is water treatment processes in which MF, UF and RO membranes are used. Despite the advantages of membrane processes, the application of these processes is limited due to the fouling phenomenon in membranes. The membrane fouling phenomenon leads to a dramatic decline in flux through the membrane [1, 2] and consequently, operating pressure should be increased to compensate the permeate flux decline, which results in higher energy demand and operational cost [3-5].

Due to the hydrophobic characteristics, most of the polymeric membranes show low water permeability and are susceptible to fouling. Therefore, many efforts have been devoted to reduce fouling in hydrophobic

* Corresponding Author - E-mail: yjafarzadeh@sut.ac.ir

polymer membranes. In order to increase the hydrophilicity of membranes, three different approaches have been generally described in the literature including pre-modification of polymers before membrane synthesis [6], incorporation of inorganic and/or organic additives during membrane preparation [1, 7, 8] and post-modification of membrane surface via different methods such as plasma surface treatment and dip-coating [9, 10]. Incorporation of inorganic particles into membranes has attracted most attentions because of the simplicity and the absence of any additional steps in the membrane preparation process [11]. Several studies have been conducted recently on embedding inorganic nanoparticles into polymer membranes to be used in different membrane-based water and wastewater treatment processes. The most important inorganic particles used in this field are TiO_2 [12, 13], nanodiamonds (NDs) [14] SiO_2 [15], graphene oxide [16,17], carbon nanotubes [18, 19] and ZnO [1, 20]. In most cases, incorporation of these particles has resulted in an improvement in performance and antifouling properties of membranes.

Polyethylene (PE) membranes are widely used in different membrane processes such as membrane distillation, membrane extraction and water treatment due to their excellent mechanical strength, chemical resistance and thermal stability [21-23]. In addition, polyethylene membrane is widely used in lithium ion batteries as separator and strong efforts are being done in this application [24]. PE membranes, however, suffer from non-wettability and poor biocompatibility due to the nonpolar nature of PE chains and therefore, their application in separation of aqueous solutions, biomedical fields and water treatment [22, 25, 26] is limited. In other word, polyethylene membranes are very susceptible to fouling [27, 28], because of the nonpolar backbone of PE and its inherent hydrophobicity. Therefore, incorporation of hydrophilic particles seems to be an effective manner to increase antifouling properties of PE membranes.

Jafarzadeh et al. prepared TiO_2 and ZnO embedded PE membranes and showed that the presence of TiO_2 and ZnO improved the performance and antifouling properties of PE membranes as well as their mechanical and thermal properties [8, 29-31]. In another work, pure and polyethylene-grafted silica nanoparticles (PEG-*g*-silica NPs) were dispersed into HDPE membranes and the results showed that the agglomeration of silica nanoparticles in the HDPE membrane decreased noticeably in comparison to that in the neat silica/HDPE membrane, resulting in higher flux and lower fouling [32]. In this research, we prepared and characterized glass fiber/HDPE composite membranes in continuation with our previous works. The basis of glass fiber is silica (SiO_2) which has been widely used as hydrophilic nanoparticles in inorganic incorporated membranes to improve antifouling properties of membranes [15, 32-34]. Glass fiber has also been recently used to reinforce the polymer matrices due to its good thermal stability and high mechanical strength [35]. Moreover, its low cost in comparison with SiO_2 nanoparticles makes it an interesting substitute for SiO_2 in composite membranes. Therefore, we expected that incorporation of glass fiber into PE membranes would improve the fouling resistance and abrasion resistance of the membranes.

EXPERIMENTAL

Material

A commercial grade high density polyethylene (X3; MW=119,500 g/mol) was provided by Amirkabir Petrochemical Company. Ultra-short glass fiber (USGF) of the length of 40-50 μm and the diameter of 10 μm was provided by Owens Corning Co. Mineral oil (MO) as diluent, acetone as extractant and dicumyl peroxide were purchased from Acros Organics, Merck and Sigma Aldrich, respectively. Silicon carbide particles of 325 and 400 mesh were purchased from Acros Organics and Sigma, respectively. BSA as protein was purchased from Merck. All materials were used as received without further purification.

Grinding the glass fiber

large USGF particles (approximately 150 μm in length and 5 μm in diameter) were grinded using a planetary ball mill (NARYA-MPM 250 H) to disperse uniformly throughout fabricated membranes. SEM images of USGF and grinded glass fiber (GGF) particles are shown in Figure 1.

Preparation of the membranes

Thermally induced phase separation method was used to prepare membranes. Before preparation of membranes, different amounts of HDPE and GGF were dried in an oven at 65°C to avoid the harmful effect of moisture and then blended together with dicumyl

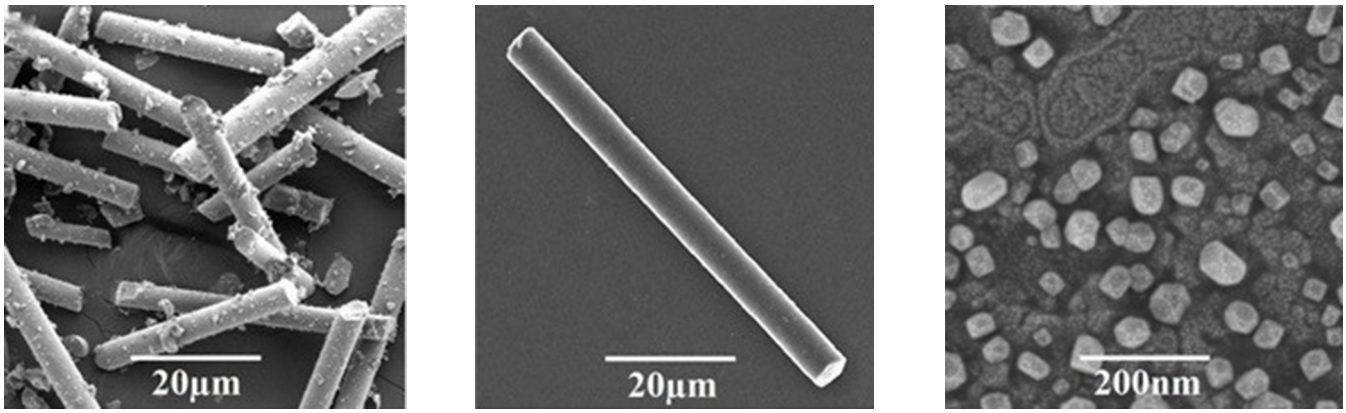

(a) (b) (c)

Figure 1. FESEM images of ultra-short glass fiber (USGF) and grinded glass fiber (GGF): (a, b) USGF, (c) GGF.

peroxide in an internal mixer (Brabender W50EHT) with a rotor speed of 60 rpm at temperature of 165°C. The weight ratio of GGF/HDPE was kept in 2.5, 5.0, 7.5 and 10.0. The blend was extruded and 12.5 g of each extruded composite was chopped and added to 50 g of MO and melt-blended at 160°C and 450 rpm for 90 min in a sealed glass vessel kept in a silicon oil bath. The solution was then allowed to degas for 30 min and cast on a preheated glass sheet using a doctor blade. The plate was immediately immersed in the water bath (30°C ±3) to induce phase separation. Finally, the membrane was immersed in acetone for 24 h and dried at room temperature to remove acetone. In addition, 2.5 wt/wt USGF/HDPE membrane was fabricated in the same procedure to show the dispersion of original glass fiber in the membrane. In the case of neat polyethylene membrane, MO and polyethylene were melt-blended at 160°C for 90 min in a sealed glass vessel kept in a silicon oil bath. The other procedures were the same as the GGF embedded membranes preparation process. The compositions of the prepared membranes are shown in Table 1.

Membrane characterization

The morphology of the membranes was characterized by FESEM (MIRA3 FEG-SEM, Tescan). Cross-section samples were prepared by fracturing the membranes in liquid nitrogen. All samples were coated with gold by sputtering before observation to make them conductive. The FESEM device was equipped with a dispersive X-ray analysis (EDX) detector to inspect the existence of glass fiber particles in the membranes. Thermal behavior and dispersion quality of grinded glass fiber particles in the fabricated membranes were investigated using a Perkin Elmer Pyris Diamond TG/DTA system at a heating rate of 20°C/min under nitrogen atmosphere. Samples were taken from three different areas of each membrane and the amount of residue was measured and reported as average of three tests. Fourier transform infrared spectroscopy (FTIR) was recorded using a Tensor 27 FTIR spectrometer (Bruker, Germany). Hydrophilicity of the membranes was evaluated by measuring the static contact angle between membrane surface and water droplet using a contact angle goniometer (PGX, Thwing-Albert Instrument Co.) at 27°C. The average of 5 measurements was reported to minimize the experimental errors. Atomic force microscopy (AFM) studies were conducted in tapping mode using Nanosurf Mobile S. Samples were prepared by cutting the membranes longitudinally in very narrow ribbons of less than 1 mm width and 5 mm length. The surface roughness of membranes (Ra) was calculated using a method mentioned elsewhere [15]. Tensile strength was determined using a tensile testing machine (STM-5, Santam) at an extension rate of 10 mm/min. Samples were cut in 50 mm length and 10 mm width. Each membrane was tested at least 3 times and averaged values were reported. Pure water flux of membranes was determined using an in-house fabricated dead-end filtration system having 5 cm^2 of membrane area. To minimize compaction effects, the pre-wetted membranes were compacted for 30 min at 2 bar. Then the pressure was reduced to 1.4 bar and after reaching steady state, water flux was calculated using the following equation:

$$J_0 = \frac{M}{A.t} \quad (1)$$

where J_0 is the pure water flux, M is the collected mass of water (kg), A is the membrane area (m^2), and t is the time (h).

Abrasion resistance testing

To examine abrasion resistance of the membranes, an accelerated testing setup was designed similar to that described in Ref. [36]. 500 g of an abrasive slurry containing 10 wt% of each silicon carbide in deionized water was placed in a baker. A 4 × 4 piece of each type of membrane was secured in the baker and immersed into slurry as shown in Figure 2. The slurry was then stirred for 7 days allowing the membrane to be in contact with abrasive silicon carbide at 500 rpm in order to provide maximum abrasion condition. The weights of the membranes were measured before and after abrasion test to determine weight loss during the test.

Fouling analysis

In order to study the effect of glass fiber on the membranes fouling behavior, the membranes were tested in a dead-end filtration system filled with BSA protein solution as a model solution. The solution was prepared by dissolving 1.00 g BSA powder in 1 L standard (0.1 M) phosphate buffer saline (PBS) solution at pH 7.2. The system consisted of a cup connected to an N_2 balloon and equipped with a stirrer. After measuring pure water flux (as mentioned earlier), the membrane holder was connected to the protein filtration system and the system was pressurized. All the filtration experiments were conducted at a trans-membrane pressure of 1.4 bar. After about 300 min filtration, the membrane cell was again connected to the pure water filtration system and pure water flux after fouling (J_1) was measured using Eq. 1. Then the cake layer on the membrane was gently removed mechanically by a sponge, and the membrane was rinsed and backwashed with deionized water at the same pressure. Finally, the membrane was held in the holder and connected to the pure water filtration system, and pure water flux after rinsing (J_2) was measured using Eq. 1. Comparison between J_0, J_1 and J_2 gives useful information about flux behavior and variety of fouling resistance of membranes. The total fouling ratio (TFR) of a membrane is defined as follow:

$$TFR = \left(\frac{J_0 - J_1}{J_0}\right) \times 100 \quad (2)$$

TFR is a degree of total flux loss caused by total fouling and the less TFR value shows the better antifouling performance for a membrane. Moreover, two other important fouling ratios are reversible fouling ratio (RFR) and irreversible fouling ratio (IFR) which can be defined by the following equations:

$$RFR = \left(\frac{J_2 - J_1}{J_0}\right) \times 100 \quad (3)$$

$$IFR = \left(\frac{J_0 - J_2}{J_0}\right) \times 100 \quad (4)$$

Finally, having J_0 and J_2, the flux recovery (FR) can be calculated easily as follow:

$$FR = \left(\frac{J_2}{J_0}\right) \times 100 \quad (5)$$

The flux recovery is an index of antifouling property of membranes. Generally, higher FR indicates that the membrane is more fouling-resistant.

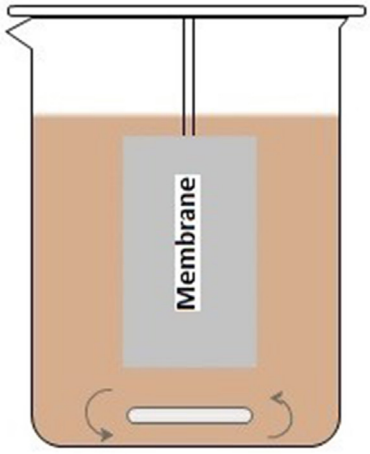

Figure 2. Abrasion test setup.

RESULTS AND DISCUSSION

FESEM, EDX, FTIR and TGA

FESEM analysis was carried out to study the morphological structure of the fabricated membranes. Images of cross-section for the membranes are shown in Figure 3. The leafy structure observed in the cross sections indicates the solid-liquid mechanism is occurred during phase separation of polymer solution. It has been shown that HDPE/MO casting solutions with compositions in the range of 15-50 wt% HDPE undergo solid-liquid phase separation and therefore, they

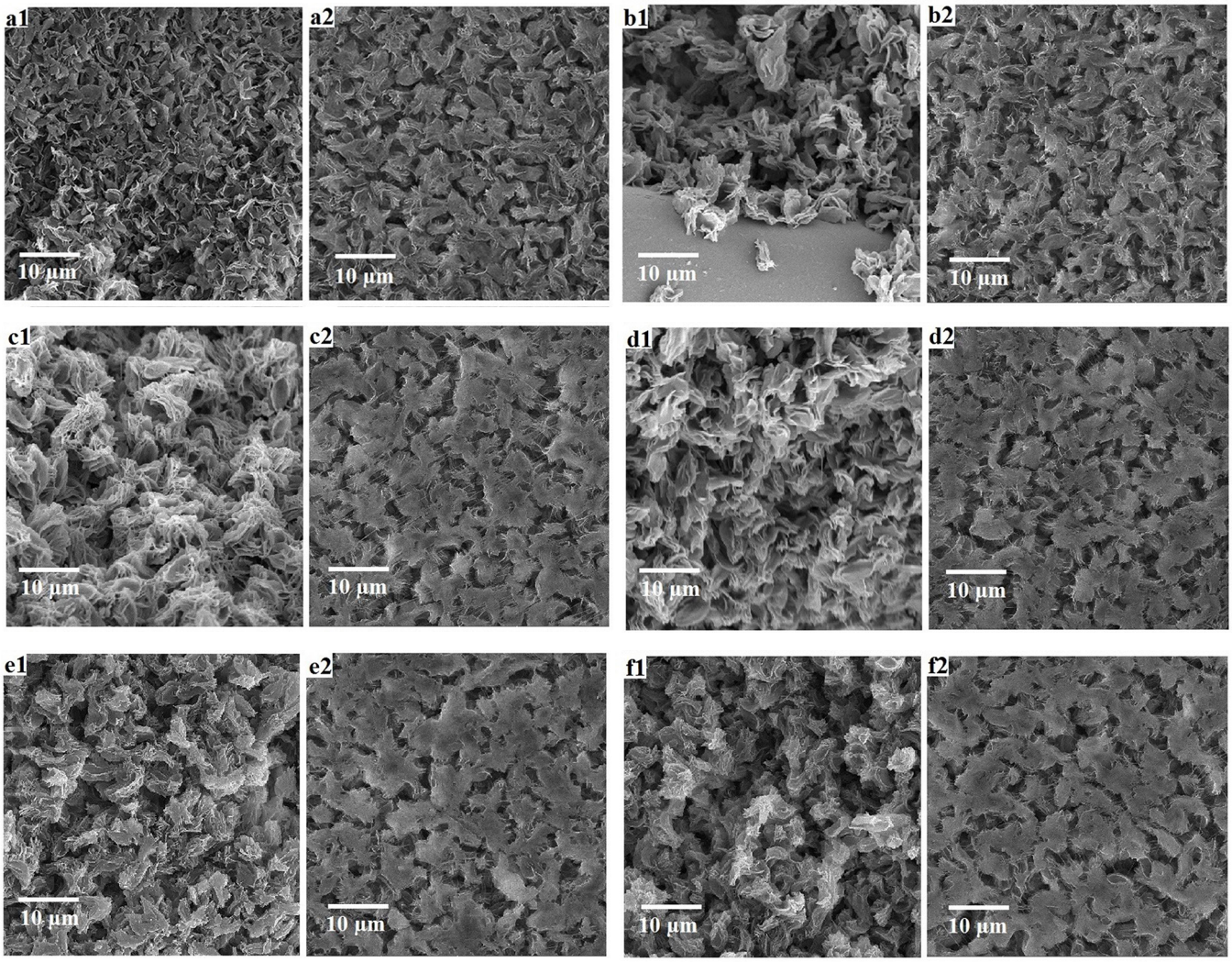

Figure 3. FESEM images of neat, USGF and GGF embedded HDPE membranes. (1) Cross sections, (2) Upper surfaces. (a) Neat HDPE membrane, (b) 2.5 wt. % USGF, (c) 2.5 wt. % GGF, (d) 5.0 wt. % GGF, (e) 7.5 wt. % GGF, (f) 10 wt. % GGF.

are capable of producing membranes with leafy structures [37]. It can be seen that the leaves are smoother in the neat HDPE membrane while the flatness of them decreases as the content of glass fiber particles increases. This may be due to the nucleation effect of glass fiber particle where the PE chains were crystalized around the nuclei during quenching step, making the structure less uniform. The observed structures were in good agreement with our previous findings [8, 29], however larger pores in membrane surfaces were obtained in the present work which may be related to the difference in size and nature of particles (TiO_2, ZnO and glass fiber). As shown in Figure 3-b1, there is a desirable interaction between glass fiber and membrane because of presence of vinyl functional group on the particles, nevertheless increasing the dosage of glass fiber to 5.0 wt.% (Figure 3-d) has resulted in destruction of the leafy structure of membrane due to larger size of glass fiber particles.

The presence of glass fiber particles in the membrane structure was also confirmed by EDX analysis. The result of EDX analysis for 10.0 wt% GGF embedded HDPE membranes is shown in Figure 4, which confirms the presence of glass fiber in the hybrid membrane. The same results were observed for 2.5, 5.0 and 7.5 wt% GGF embedded HDPE membranes (data are not shown).

Figure 5 shows FTIR analysis of pure nanoparticles as well as pure HDPE and composite membranes. In FTIR spectra, the absorption peak at 720-740 cm^{-1} is assigned to the $-(CH_2)_n-$ in HDPE samples.

In comparison with pure HDPE membrane, the composite membranes show new absorption peak at 1410cm^{-1} corresponding to $Si–CH=CH_2$ (vinyl group). Also, the very broad peak between 3600 and 3100cm^{-1} indicates the presence of OH group in the composite

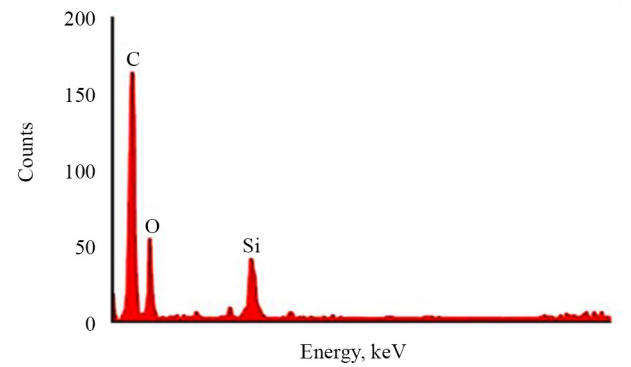

Figure 4. The EDX result of 10 wt. % GGF embedded HDPE membrane.

membrane due to the existence of glass fiber.

According to the method presented by Razmjou et al. [41], TGA analysis was used to confirm the homogenous distribution of grinded glass fiber in the membranes. For each membrane three pieces from different parts of a flat sheet membrane were cut and used. Figure 6 shows the obtained results for the membranes. It can be seen that, for example, the residue for 5.00 wt% GGF embedded HDPE membrane is 4.37% (close to the expected value of 5.00%) which indicates that GGF was well dispersed throughout the membrane. It should be noted that the presence of all of the particles in the final membrane is not possible because some particles c leach out during membrane fabrication process. Therefore, the amount of particles in the membrane is always lower than its theoretical value and the difference between these values is reasonable. Thus, the results confirm good dispersion of glass fiber in the membranes as well as insignificant loss of nanoparticles during membrane fabrication process. The same set of experiments was conducted for other membranes and the results were summarized in Table 2.

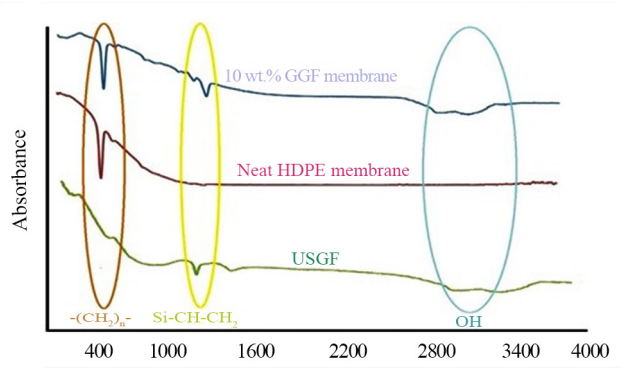

Figure 5. FTIR spectra of USGF, neat HDPE membrane and 10 wt. % GGF embedded HDPE membranes.

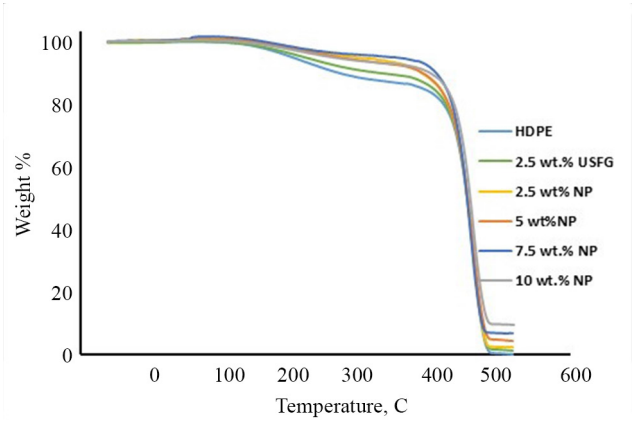

Figure 6. TGA thermograms of neat and glass fiber embedded HDPE membranes.

Surface characteristics of membranes

The contact angle is a measurement of the affinity for the water droplets to wet the solid surface. The lower contact angle means the greater wettability and the higher hydrophilicity. Figure 7 shows the contact angle for the fabricated membranes. There is a relative reduction in contact angle from 128° for neat HDPE membranes to 95° for 10 wt% reinforced membrane due to hydrophilic nature of glass fiber associated with hydrophilic SiO_2. Decrease in contact angle is mainly due to the presence of a large number of hydroxyl groups on the chemical structure of SiO_2 particles [32]. Cui et al. showed that the introduction of SiO_2 particles increased the hydrophilicity of PVDF membranes [15]. The same result was obtained by X. Zuo et al. who prepared SiO_2/PVDF membranes [39]. Also, decrease in the contact angle in the presence of inorganic particles has been reported in other studies [8, 29]. Comparing Figure 7-b with Figure 7-c, it was illustrated that grinding the USGF particles could significantly improve the hydrophilicity of fabricated membranes.

Figure 8 shows the three-dimensional images of the

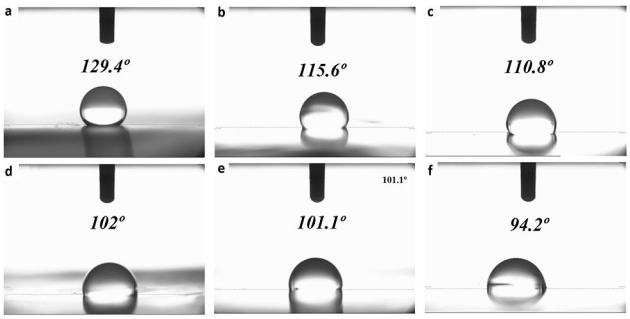

Figure 7. Contact angle images of fabricated membranes: (a) Neat HDPE membrane, (b) 2.5 wt. % USGF, (c) 2.5 wt. % GGF, (d) 5.0 wt. % GGF, (e) 7.5 wt. % GGF, (f) 10 wt. % GGF.

outer surface of membranes. It can be seen that the surface roughness of membranes increases as the content of glass fiber particles increases, which may be as a result of particles accumulation on the membrane surface by increasing SiO_2 particles [40]. In the range of scan area of 8 µm × 8 µm, the surface roughness of the neat, 2.5 wt% USGF, 2.5, 5.0, 7.5 and 10.0 wt% GGF embedded HDPE membranes were 63.17, 82.66, 90.04, 110.21, 127.81 and 141.93 nm, respectively. Increasing the surface roughness with incorporation of inorganic particles has also been reported in other studies [32, 40] and the same results were obtained in our previous works [8, 29]. The surface roughness characteristics seriously affect the adsorption/desorption of foulants on the membrane surface which can control the membrane fouling. As will be discussed later, the antifouling property of membranes would be potentially affected by surface roughness of membranes.

Pure water flux and mechanical strength

The effect of glass fiber loading on the water flux was investigated, and the results are presented in Figure 9. It can be seen that PWF of the membranes enhances as the content of glass fiber increases up to 5 wt%. Several factors involving hydrophilicity, surface pore size and cross section structure can affect pure water flux of the membranes. As shown in Figure 7, the presence of glass fiber particles has led to a decline in the water contact angle and an improvement in the hydrophilicity of the membranes due to the higher affinity of glass fiber to water. In other words, the presence of hydrophilic glass fiber particles facilitates the sorption of water on the membrane surface and consequently,

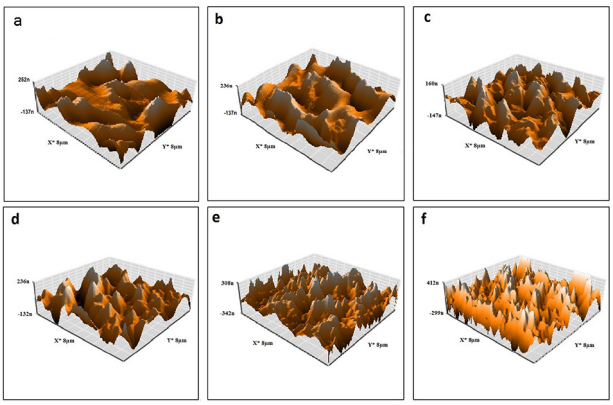

Figure 8. AFM images of prepared membranes: (a) Neat HDPE membrane, (b) 2.5 wt. % USGF, (c) 2.5 wt. % GGF, (d) 5.0 wt. % GGF, (e) 7.5 wt. % GGF, (f) 10.0 wt. % GGF.

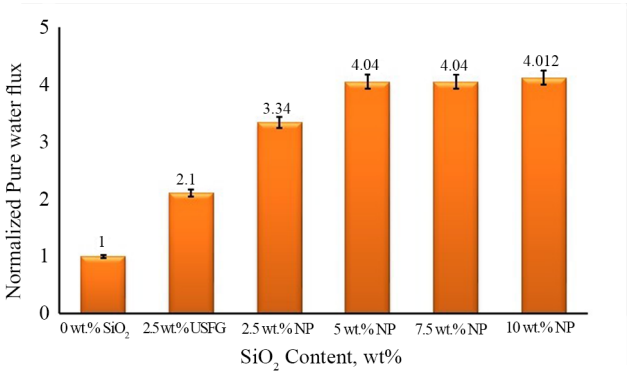

Figure 9. Normalized pure water flux of prepared membranes.

within the internal pores of the membrane. Therefore, it is expected that increasing the membrane hydrophilicity leads to improve the pure water flux.

However, at the higher contents of glass fiber (7.5 and 10.0 wt%), the water flux became almost invariant. As the glass fiber content increased from 5 to 10 wt%, the water permeation resistance increased due to the agglomeration of particles which may impede the permeation of water through the membrane. Therefore, agglomeration of glass fiber particles at the higher contents compensates the hydrophilicity of them, resulting in no change in pure water flux of the membranes.

The addition of inorganic particles into a polymer alters the mechanical properties of polymer [41]. Tensile strength-at-break is an important parameter to describe the mechanical behavior of membranes. Figure 10 shows that incorporation of GGF into HDPE membranes up to 5.0 wt% improves tensile strength which is mainly due to the reinforcement effect of the inorganic nanoparticles along with crosslinking caused by dicumyl peroxide. Moreover, the attachment of GGF to the HDPE chains could enhance the mechanical strength to some extent. As shown in the FTIR analy-

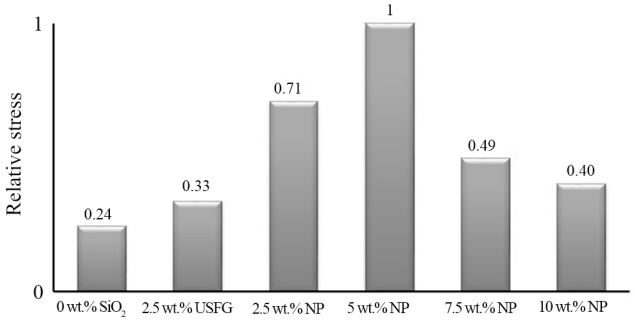

Figure 10. Normalized tensile strength of prepared membranes.

sis, the Si–CH=CH_2 bond is observed in the glass fiber incorporated membranes, indicating that dicumyl peroxide acts as an attachment agent between the polymer chains and inorganic glass, which may bear the stress and consequently, improve the mechanical properties of the glass fiber incorporated membranes. However, at the higher content of GGF the mechanical tensile strength decreased, which could be mainly related to agglomeration of GGF particles at the higher content.

Abrasion resistance

FESEM images of the membrane surface after abrasion test are shown in Figure 11. The results show that the HDPE membrane reveals the most worn and damaged surface after abrasion testing for both 325 and 400 silicon carbide particles, whereas the composite membranes are less sensitive to abrasive materials. This implies that incorporation of GGF into the HDPE membranes increases the abrasion resistance of the composite membranes which may be attributed to the reinforcement effect of inorganic glass fiber within the HDPE matrix. Moreover, the results show that membranes are more sensitive to silicon carbide 325 than 400 which is related to their average particle size. The particle size range of the former is 44-50 µm and the latter is 34-38 µm. Therefore, silicon carbide 325 is more abrasive and rougher compare with silicon carbide 400.

To have a quantitative view of the abrasion test, the weight loss per unit area as well as reduction in the tensile strength of membranes were measured after the test and the results are depicted in Figures 12 and 13, respectively. Figure 12 shows that all the composite membranes demonstrate a lower weight loss than the neat HDPE membrane. For example, in the abrasion test with using silicon carbide 325, 7.5 wt% GGF in-

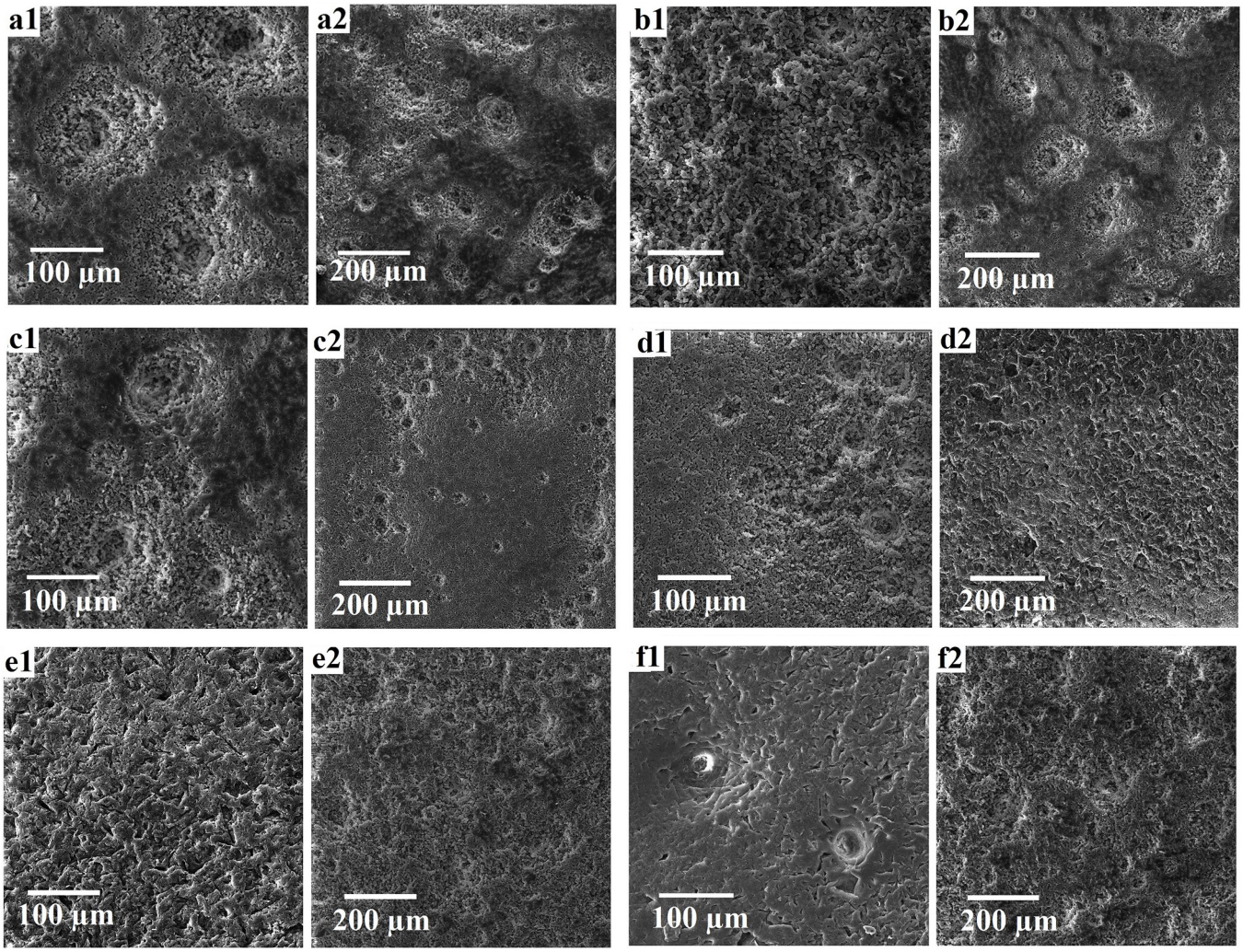

Figure 11. FESEM images of membrane surface after abrasion test. (1) Silicon carbide 400, (2) Silicon carbide 325, (a) Neat HDPE membrane, (b) 2.5 wt. % USGF, (c) 2.5 wt. % GGF, (d) 5.0 wt. % GGF, (e) 7.5 wt. % GGF, (f) 10 wt. % GGF.

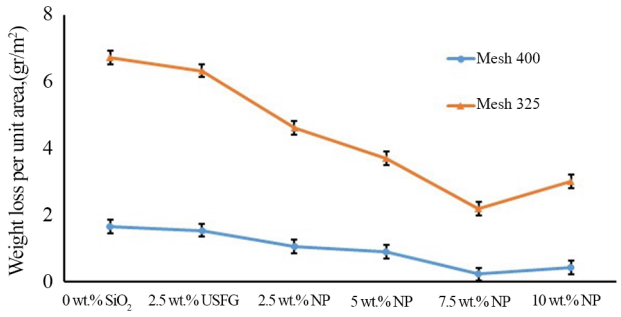

Figure 12. Weight loss per unit area of membrane after 7 days abrasion test with two different silicon carbide particles.

corporated membrane lost 2.2 g/m^2 whereas the neat HDPE membrane lost 6.7 g/m^2. This means that, the 7.5 wt% GGF incorporated membrane can last about three times longer than neat HDPE membrane under the same abrasive conditions.

Figure 13 shows that the tensile strength of all membranes decreases after abrasion test with silicon carbide 400. The decrease in the tensile strength for the neat HDPE membrane is more severe than that of glass fiber incorporated membranes. The tensile strength of HDPE membrane before and after abrasion test is 0.87 and 0.23 MPa, respectively which shows a 74% decrease after abrasion. However, incorporation of 5.0 wt% glass fiber into HDPE membrane increased its tensile strength up to 3.56 MPa, and it dropped to 3.27 MPa after abrasion, an 8% decrease in the tensile strength. Therefore, it can be concluded that incorporation of glass fiber into HDPE membranes has a positive effect on the mechanical properties of the membranes.

Antifouling characteristics of the membranes

Evaluation of the fouling performance of the prepared membranes was carried out by using the 1.00 g/L BSA solution based on the flux decline during BSA filtration as depicted in Figure 14. It can be seen that the initial flux of glass fiber embedded membranes is higher than that of neat HDPE membrane, and after 4 h filtration, the flux of neat HDPE membrane dropped to 42% of its initial value. In contrast, 2.5, 5.0, 7.5, and 10.0 wt% glass fiber embedded membranes preserve 73, 78, 73, and 64% of their initial fluxes, respectively. As shown in the figure, incorporation of glass fiber improves antifouling properties of the hybrid membranes which can be related to the hydrophilicity of these membranes.

Figure 15 shows TFR, RFR, IFR and FR values estimated from membrane flux during filtration of BSA solution to compare the antifouling properties of the fabricated membranes. Generally, the membrane fouling comprises reversible and irreversible fouling. The former is resulted from reversible adsorption of protein molecules on the membrane surface or within its pores and can be easily removed by cleaning method and the latter is resulted from strong adsorption of the proteins [17]. It can be seen that the neat HDPE membrane shows the highest TFR, indicating that this membrane is easily fouled by BSA molecules. Incorporation of glass fiber however, decreased TFR from 90% for neat membrane to 62% for 10.0 wt% GGF embedded membrane. Moreover, IFR of membranes decreased from 42% for neat membrane to 17% for 10.0 wt% GGF embedded membrane, even though RFR was not affected noticeably.

This indicates that the incorporation of glass fiber nanoparticles into the HDPE membranes not only increased the fouling resistance, but also decreased the irreversible fouling. Another comparison of the anti-

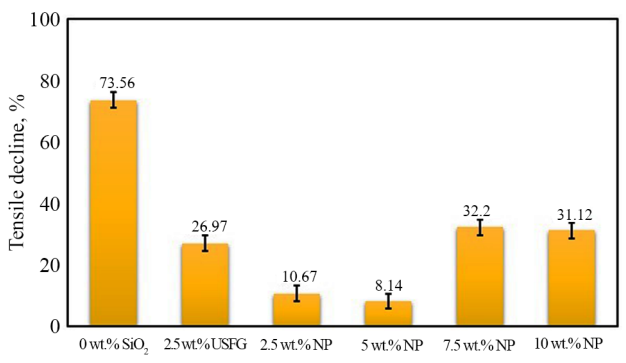

Figure 13. Tensile decline of membranes after abrasion test with silicon carbide 400.

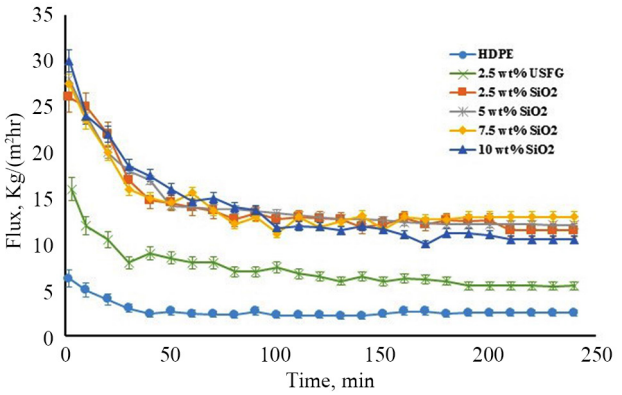

Figure 14. Flux–time behavior of neat, USGF and GGF embedded HDPE membranes in the filtration process of 1 g/L BSA solution.

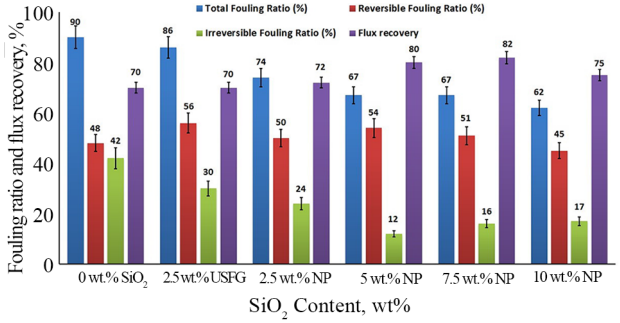

Figure 15. Fouling parameters of neat, USGF and GGF embedded HDPE membranes.

fouling properties of the membranes could be obtained by considering the FR values. From Figure 15, it can be seen that FR of the hybrid membranes were higher than that of neat HDPE membrane. The increase in the flux recovery could be attributed to the presence of glass fiber on the surface of the membranes which caused to increase the membrane hydrophilicity.

CONCLUSION

In this study, grinded glass fiber embedded HDPE membranes were prepared via thermally induced phase separation method. The results from this study showed that all of the membranes had leafy structure, indicating a solid-liquid mechanism during phase separation. The existence of glass fibers in the membranes' matrix and their uniform dispersion were confirmed by EDX and TGA analyses. It was shown that glass fiber improved the antifouling properties of the membranes. The HDPE/glass fiber membranes showed a higher water flux and a lower flux decline during filtration of BSA solution compared to the neat HDPE membranes. These findings were attributed to the hydrophilicity of glass fiber. The results of abrasion test with silicon carbide slurry revealed that the glass fiber/HDPE membranes were more abrasion resistant than the neat HDPE membrane. Tensile strength of the composite membranes before and after abrasion test was also higher than that of the neat HDPE membrane. Therefore, glass fiber embedded HDPE membranes are suitable candidate for water treatment application.

REFERENCES

1. Balta S, Sotto A, Luis P, Benea L, Van der Bruggen B, Kim J (2012) A new outlook on membrane enhancement with nanoparticles: The alternative of ZnO. J Membrane Sci 389: 155-161
2. Hilal N, Ogunbiyi OO, Miles NJ, Nigmatullin R (2005) Methods employed for control of fouling in MF and UF membranes: A comprehensive review. Separ Sci Technol 40: 1957-2005
3. Hoek EMV, Ghosh AK, Huang X, Liong M, Zink JI (2011) Physical-chemical properties, separation performance, and fouling resistance of mixed-matrix ultrafiltration membranes. Desalination 283: 89-99
4. Van der Bruggen B, Braeken L, Vandecasteele C (2002) Flux decline in nanofiltration due to adsorption of organic compounds. Sep Purif Technol 29: 23-31
5. Van der Bruggen B, Manttari M, Nystrom M (2008) Drawbacks of applying nanofiltration and how to avoid them: A review. Sep Purif Technol 63: 251-263
6. Ulbricht M (2006) Advanced functional polymer membranes. Polymer 47: 2217-2262
7. Liang S, Xiao K, Mo Y, Huang X (2012) A novel ZnO nanoparticle blended polyvinylidene fluoride membrane for anti-irreversible fouling. J Membrane Sci 394: 184-192
8. Jafarzadeh Y, Yegani R (2015) Analysis of fouling mechanisms in TiO_2 embedded high density polyethylene membranes for collagen separation. Chem Eng Res Des 93: 684-695
9. Rahimpour A, Madaeni SS, Taheri AH, Mansourpanah Y (2008) Coupling TiO_2 nanoparticles with UV irradiation for modification of polyethersulfone ultrafiltration membranes. J Membrane Sci 313: 158-169
10. Ulbricht M, Belfort G (1996) Surface modification of ultrafiltration membranes by low temperature plasma II. Graft polymerization onto polyacrylonitrile and polysulfone. J Membrane Sci 111: 193-215
11. De Sitter K, Dotremont C, Genne I, Stoops L (2014) The use of nanoparticles as alternative pore former for the production of more sustainable polyethersulfone ultrafiltration membranes. J Membrane Sci 471: 168-178
12. Shi F, Ma Y, Ma J, Wang P, Sun W (2012) Preparation and characterization of PVDF/TiO_2 hybrid membranes with different dosage of nano-TiO_2. J Membrane Sci 389: 522-531

13. Behboudi A, Jafarzadeh Y, Yegani R (2016) Preparation and characterization of TiO_2 embedded PVC ultrafiltration membranes. Chem Eng Res Des 114: 96-107
14. Etemadi H, Yegani R, Babaeipour V (2016) Study on the reinforcing effect of nanodiamond particles on the mechanical, thermal and antibacterial properties of cellulose acetate membranes. Diamond Relat Mater 69: 166-176
15. Cui A, Liu Z, Xiao C, Zhang Y (2010) Effect of micro-sized SiO_2-particle on the performance of PVDF blend membranes via TIPS. J Membrane Sci 360: 259-264
16. Safarpour M, Khataee A, Vatanpour V (2015) Thin film nanocomposite reverse osmosis membrane modified by reduced graphene oxide/TiO_2 with improved desalination performance. J Membrane Sci 489: 43-54
17. Zhang J, Xu Z, Shan M, Zhou B, Li Y, Li B, Niu J, Qian X (2013) Synergetic effects of oxidized carbon nanotubes and graphene oxide on fouling control and anti-fouling mechanism of polyvinylidene fluoride ultrafiltration membranes. J Membrane Sci 448: 81-92
18. Wang L, Song X, Wang T, Wang S, Wang Z, Gao C, (2015) Fabrication and characterization of polyethersulfone/carbon nanotubes (PES/CNTs) based mixed matrix membranes (MMMs) for nanofiltration application. Appl Surf Sci 330: 118-125
19. Zhang Q, Veciti CD, (2014) Conductive CNT-PVDF membrane for capacitive organic fouling reduction. J Membrane Sci 459: 143-156
20. Rabiee H, Vatanpour V, Davood Abadi Farahani MH, Zarrabi H, (2015) Improvement in flux and antifouling properties of PVC ultrafiltration membranes by incorporation of zinc oxide (ZnO) nanoparticles. Sep Purif Technol 156: 299–310
21. Xi Z-Y, Xu Y-Y, Zhu L-P, Du C-H, Zhu B-K (2008) Effect of stretching on structure and properties of polyethylene hollow fiber membranes made by melt-spinning and stretching process. Polym Advan Technol 19: 1616-1622
22. Zhang C, Bai Y, Sun Y, Gu J, Xu Y (2010) Preparation of hydrophilic HDPE porous membranes via thermally induced phase separation by blending of amphiphilic PE-b-PEG copolymer. J Membrane Sci 365: 216-224
23. Kolesov IS, Kratz K, Lendlein A, Radusch H-J(2009) Kinetics and dynamics of thermally-induced shape-memory behavior of crosslinked short-chain branched polyethylenes. Polymer 50: 5490-5498
24. Park MJ, Kim CK (2014) Fabrication of polyethylene microporous membranes using triethylolpropane tris(2-ethylhexanoate) as a novel diluent by a thermally induced phase separation process. J Membrane Sci 449: 127-135
25. Mosadegh-Sedghi S, Rodrigue D, Brisson J, Iliuta MC (2013) Highly hydrophobic microporous low-density polyethylene hollow fiber membranes by melt-extrusion coupled with salt-leaching technique. Polym Adv Technol 24: 584-592
26. Liu J-H, Jen H-L, Chung Y-C (1999) Surface modification of polyethylene membranes using phosphorylcholine derivatives and their platelet compatibility. J Appl Polym Sci 74: 2947-2954
27. Zhang J, Jiang DD, Wilkie CA (2006) Polyethylene and polypropylene nanocomposites based on a three component oligomerically-modified clay. Polym Degrad Stabil 91: 641-648
28. Zhang J, Jiang DD, Wilkie CA (2005) Polyethylene and polypropylene nanocomposites based upon an oligomerically modified clay. Thermochim Acta 430: 107-113
29. Jafarzadeh Y, Yegani R, Sedaghat M (2015) Preparation, characterization and fouling analysis of ZnO/polyethylene hybrid membranes for collagen separation. Chem Eng Res Des 94: 417-427
30. Jafarzadeh Y, Yegani R (2015) Thermal, mechanical, and structural properties of ZnO/polyethylene membranes made by thermally induced phase separation method. J Appl Polym Sci 132: 42338
31. Jafarzadeh Y, Yegani R, Tantekin-Ersolmaz SB (2015) Effect of TiO_2 nanoparticles on structure and properties of high density polyethylene membranes prepared by thermally induced phase separation method. Polym Advan Technol 26: 392-398
32. Peyki A, Rahimpour A, Jahanshahi M (2015) Preparation and characterization of thin film composite reverse osmosis membranes incorporated with hydrophilic SiO_2 nanoparticles. Desalination 368: 152-158
33. Ghandashtani MB, Zokaee Ashtiani F, Karimi M, Fouladitajar A (2015) A novel approach to fabricate high performance nano-SiO_2 embedded PES membranes for microfiltration of oil-in-water

emulsion. Appl Surf Sci 349: 393-402
34. Efome JE, Baghbanzadeh M, Rana D, Matsuura T, Lan CQ (2015) Effects of superhydrophobic SiO_2 nanoparticles on the performance of PVDF flat sheet membranes for vacuum membrane distillation. Desalination 373: 47-57
35. Luo N, Xu R, Yang M, Yuan X, Zhong H, Fan Y (2015) Preparation and characterization of PVDF-glass fiber composite membrane reinforced by interfacial UV-grafting copolymerization, J Environ Sci 38: 24-35
36. Lai CY, Groth A, Gray S, Duke M (2014) Enhanced abrasion resistant PVDF/nanoclay hollow fiber composite membranes for water treatment. J Membrane Sci 449: 146-157
37. Lloyd DR, Kinzer KE, Tseng HS (1990) Microporous membrane formation via thermally induced phase separation. I. Solid-liquid phase separation. J Membrane Sci 52: 239-261
38. Razmjou A, Mansouri J, Chen V (2011) The effects of mechanical and chemical modification of TiO_2 nanoparticles on the surface chemistry, structure and fouling performance of PES ultrafiltration membranes. J Membrane Sci 378: 73-84
39. Zuo X, Wang L, He J, Li Z, Yu S (2014) SEM-EDX studies of SiO_2/PVDF membranes fouling in electrodialysis of polymer-flooding produced wastewater: Diatomite, APAM and crude oil. Desalination 347: 43-51
40. Kebria MRS, Jahanshahi M, Rahimpour A (2015) SiO_2 modified polyethyleneimine-based nanofiltration membranes for dye removal from aqueous and organic solutions. Desalination 367: 255-264
41. Nguyen VG, Thai H, Mai DH, Tran HT, Tran DL, Vu MT (2013) Effect of titanium dioxide on the properties of polyethylene/TiO_2 nanocomposites. Composites Part B- Eng 45: 1192-1198